A numerical study on continuous space-time Finite Element Methods for dynamic Signorini problems

Andreas Rademacher

Institute of Applied Mathematics, Technische Universität Dortmund

Abstract

Space-time finite element methods for dynamic Signorini problems are discussed in this article. The discretization scheme is based on a mixed space-time formulation of the continuous problem, where the Lagrange multipliers represent the contact stress. To construct the trial space for the displacement and the velocity, we use piecewise polynomial and globally continuous basis functions in space and time. It is combined with a test space consisting of piecewise polynomial and possibly discontinuous basis functions in time. The Lagrange multiplier is approximated by piecewise discontinuous polynomials in space and time. By suitable combinations of the polynomial degrees as well as the underlying meshes, we ensure the stability of the presented scheme, which is substantiated by some numerical experiments.

Keywords: Dynamic Signorini problem, continuous space-time finite element method, mixed method

1 Introduction

Dynamic contact problems play an important role in many engineering processes. We exemplify grinding processes here. The contact of the tool and the workpiece is typically the main source of dynamic deflections of the grinding machine, where the contact arises only in a small area. Consequently, it is essential in the simulation of such processes to use an accurate and reliable numerical scheme to approximate the contact. We refer to [47] for an elaborated description of a grinding process and the corresponding simulation approach.

The inclusion of geometrical and frictional constraints leads to inequality conditions in addition to the usual systems of partial differential equations arising from the modeling of mechanical processes, cf. [31, 36, 49]. The numerical solution of dynamic contact problems is a challenging task and a huge number of approaches are presented in literature. We refer to the monographs [36, 49] and the survey articles [18, 35] for an overview. Usually, finite difference schemes are used for the discretization of the temporal direction and finite element methods are applied for the approximation of the spatial problems. In general, Rothe's method is employed, i.e. the temporal variable is discretized first. Discretization schemes for dynamic contact problems using special parameters in the Newmark [39] or in the generalized-α method [12] are proposed in [5, 13, 46]. An important topic during the discretization is the conservation of energy and momentum. Discretization methods based on these conservation properties are developed in [3, 37]. A second crucial issue are arising oscillations in the contact forces. One approach to circumvent these oscillations but preserving energy conservation is to redistribute the mass in the system by changing the mass matrix. In [30], the mass matrix is modified by optimization algorithms, whereas special quadrature rules are used in [21]. A complete implicit treatment of the contact constraints is implemented in the Newmark method in [28, 29]. This scheme is stable but energy dissipative. Using a modified predictor step in

the Newmark method, an L^2-projection of the predicted displacement on the admissible set, a stable scheme is introduced in [15, 34], which is only slightly energy dissipative. Furthermore, a consistency result and an adaptive time stepping for this method are presented in [32]. Space adaptive discretizations are discussed in [8, 9]. A penalty method to solve dynamic contact problems is developed in [45]. Special finite elements to smooth the contact forces are applied in [38, 41]. A Nitsche finite element method for dynamic contact problems is proposed in [10, 11].

The time discretization leads to a sequence of semi-discrete contact problems, which are similar to static contact problems. Consequently, the same solution techniques are applied. Concerning the numerical solution of static contact problems, a huge number of contributions exist. Again, we refer to the monographs [36, 49]. This field of research is still an important subject and we refer to the recent works [16, 26, 27, 33, 48]. We employ the techniques developed in [17, 22, 23, 24] and extended to higher order finite elements in [7, 43, 44].

In this article, we focus on the holistic discretization of dynamic contact problems, i.e. the temporal and spatial discretization are carried out simultaneously. This approach allows for the consideration of space-time effects in a simpler way. Thus, the analysis of the approach is simpler and provides more inside in the interaction of space and time. Our approach relies on a mixed formulation in space-time, which is explained in Section 2. After the introduction of the continuous problem formulation, we present the higher order finite element scheme in more detail. Globally continuous basis functions in space and time are used to form the trial space for the displacement and the velocity. The corresponding test space consists of possibly discontinuous basis functions in time but globally continuous ones in space. The Lagrange multiplier is discretized by possibly discontinuous basis functions in space and time. We proof in Section 3 that this approach is energy conserving. The choice of a discontinuous test space is crucial for this discretization, because it enables us to decouple the single time intervals and to derive a time stepping scheme, cf. Section 4. The arising discrete problem in every time step has the same structure as static contact problems and is solved by the techniques presented in [7]. In [44], it was shown that the higher order mixed method for contact problems is stable, if the quotient of the polynomial degree of the displacement and of the Lagrange mutiplier times the quotient of the corresponding mesh widths is sufficiently small. In Section 5, we substantiate by some numerical experiments that this result carries over to the space-time setting. Unfortunately, a second assumption for stability is found, which correlates the spatial mesh width with the time step length. We conclude the paper with a discussion of the results and an outlook on further tasks.

2 Continuous formulation

In this section, we discuss the continuous formulation of the dynamic Signorini problem. The initial point is the strong formulation, which is reformulated in the weak sense as mixed problem. The mixed formulation is the basis for the presented discretisation. The section concludes with some remarks on the analytic properties of the dynamic Signorini problem.

2.1 Strong formulation

The basic domain is $\Omega \subset \mathbb{R}^d$, $d = 2, 3$ and $I = [0, T]$ the time interval. The boundary $\partial\Omega$ of Ω is divided into three mutually disjoint parts Γ_D, Γ_C and Γ_N with positive measure. Homogeneous Dirichlet and Neumann boundary conditions are prescribed on the closed set Γ_D and on the relatively open set Γ_N, respectively. Contact may take place on the sufficiently smooth set Γ_C, $\bar{\Gamma}_C \subset \complement\Gamma_D$. See, for instance, [31, Section 5.3] for more details. The rigid

foundation is parametrized by the function

$$g : \Gamma_C \times I \to \mathbb{R} \cup \{-\infty\},$$

including a suitable linearization, cf. [31, Chapter 2].

In the description of dynamic contact problems, we assume homogeneous Neumann boundary conditions to ease the notation. A linear elastic material model is used to describe the material behaviour. The displacement is given by the function $u : \Omega \times I \to \mathbb{R}^d$ and u_n is the displacement on the boundary in the outward normal direction. In this context, $\varepsilon(u) := \frac{1}{2}\left(\nabla u + \nabla u^\top\right)$ denotes the strain and $\sigma(u) = \mathbb{C}\varepsilon(u)$ the stress. The fourth order tensor $\mathbb{C}$ only depends on the modulus of elasticity $E > 0$ and Poisson's ratio $\nu \in \left[0, \frac{1}{2}\right)$. By $\sigma_n(u)$, we denoted the stress on the surface, where we distinguish between $\sigma_{nn}(u)$, the stress on the surface in normal direction, and $\sigma_{nt}(u)$, the stress in tangential direction. Superposed dots denote temporal derivatives. The initial displacement is given by u_s and the initial velocity by v_s. The volume forces are denoted by f.

If the solution u is sufficiently smooth, for instance, $u \in C^2(\Omega \times I)$, it fulfills the equations of structural dynamics including the boundary and initial conditions

$$\begin{aligned}
\ddot{u} - \operatorname{div}(\sigma(u)) &= f && \text{in } \Omega \times I, && (1)\\
u &= 0 && \text{on } \Gamma_D \times I, && (2)\\
\sigma_n(u) &= 0 && \text{on } \Gamma_N \times I, && (3)\\
u(0) &= u_s && \text{in } \Omega, && (4)\\
\dot{u}(0) &= v_s && \text{in } \Omega, && (5)
\end{aligned}$$

as well as the contact conditions

$$\begin{aligned}
u_n - g &\leq 0 && \text{on } \Gamma_C \times I, && (6)\\
\sigma_n(u) &\leq 0 && \text{on } \Gamma_C \times I, && (7)\\
\sigma_{nn}(u)(u_n - g) &= 0 && \text{on } \Gamma_C \times I, && (8)\\
\sigma_{nn}(u)(\dot{u}_n - \dot{g}) &= 0 && \text{on } \Gamma_C \times I. && (9)
\end{aligned}$$

Henceforth, we set $\rho \equiv 1$ for notational simplicity. In comparison to the static contact case, the persistency condition (9) has been added. It corresponds to the complementarity condition (8), only the gap $u_n - g$ is replaced by the gap rate $\dot{u}_n - \dot{g}$. We see in Proposition 2 that the persistency condition ensures the conservation of energy, if no outer forces occur. Therewith, the impact is purely elastic. To clarify the meaning of the persistency condition, we examine the following equivalent form (cf. [36]) of the contact conditions (6-9) on $\Gamma_C \times I$:

$$u_n - g < 0 \quad \Rightarrow \quad \begin{cases} \sigma_{nn}(u) = 0 \\ \dot{u}_n \text{ unconstrained,} \end{cases} \tag{10}$$

$$u_n - g = 0 \quad \Rightarrow \quad \begin{cases} \sigma_{nn}(u) \leq 0 \\ \dot{u}_n - \dot{g} \leq 0 \\ \sigma_{nn}(\dot{u}_n - \dot{g}) = 0. \end{cases} \tag{11}$$

The condition (10) says that the movement of the elastic body is free, if the gap is open. If the gap is closed, then condition (11) denotes that the contact stresses are negative, which is known from the static context. But now, the gap rate has to be less than zero, too. This ensures that $u_n - g \leq 0$ holds. Furthermore, we recover the persistency condition (9).

2.2 Weak formulation

After having discussed the strong formulation, we now define the weak one. To this end, we briefly present the underlying function spaces. A detailed description of Sobolev spaces can be found, e.g., in [1]. An overview of the spaces, which are mainly used in the context of contact problems, is given in [31]. For the time dependent Sobolev spaces, see, e.g., [14, 19].

The basic function space is $L^2(\Omega)$ with the scalar product $(\omega,\varphi) := (\omega,\varphi)_\Omega := \int_\Omega \omega\varphi\, dx$ for $\omega,\varphi \in L^2(\Omega)$ and the corresponding norm $\|\omega\|_0^2 := \|\omega\|_{0,\Omega}^2 := (\omega,\omega)$. The Sobolev space $H^k(\Omega)$, $k = 1,2,\ldots$, with the norm $\|\cdot\|_k^2$ is defined as usual. We set $\mathcal{H}^k := \left(H^k(\Omega)\right)^d$, $k = 1,2,\ldots$, and $\mathcal{L}^2 := \left(L^2(\Omega)\right)^d$. The trace operator is given by $\gamma : \mathcal{H}^1 \to \left(H^{1/2}(\partial\Omega)\right)^d$ with the trace space $H^{1/2}(\partial\Omega)$.

Using the trace operator, we define

$$H_D^1(\Omega) := \left\{\varphi \in H^1(\Omega) \,|\gamma(\varphi) = 0 \text{ on } \Gamma_D\right\}, \quad \mathcal{H}_D^1 := \left(H_D^1(\Omega)\right)^d.$$

The dual space $\left(H_D^1(\Omega)\right)^\star$ is called $H^{-1}(\Omega)$ and $\left(\mathcal{H}_D^1\right)^\star = \mathcal{H}^{-1}$. The dual pairing is denoted by $\langle\cdot,\cdot\rangle$. The space $\tilde{H}^{-1/2}(\Gamma_C)$ is the topological dual space of $H^{1/2}(\Gamma_C)$. The norm connected to $\tilde{H}^{-1/2}(\Gamma_C)$ is called $\|\cdot\|_{-1/2,\Gamma_C}$. The linear and bounded mapping $\gamma_c := H^1(\Omega,\Gamma_D) \to H^{1/2}(\Gamma_C)$ with $\gamma_C = \gamma_{|\Gamma_C}$ is surjective due to the assumptions on Γ_C, cf. [31, p. 88]. Here, we distinguish between the trace in normal direction $\gamma_n(u) := \left(\gamma_{|\Gamma_C}(u)\right)_n$ and the one in tangential direction $\gamma_t(u) := \left(\gamma_{|\Gamma_C}(u)\right)_t$. For functions in $L^2(\Gamma_C)$, the inequality symbols $\geq$ and $\leq$ are defined as "almost everywhere". With this definition, we can state the spaces

$$H_-^{1/2}(\Gamma_C) := \left\{ v \in H^{1/2}(\Gamma_C) \,\middle|\, v \leq 0 \right\}$$

and

$$\tilde{H}_+^{-1/2}(\Gamma_C) := \left\{ \mu \in \tilde{H}^{-1/2}(\Gamma_C) \,\middle|\, \forall v \in H_-^{1/2}(\Gamma_C) :\ \langle \mu, v\rangle \leq 0 \right\},$$

where $\tilde{H}_+^{-1/2}(\Gamma_C)$ is the dual cone of $H_+^{1/2}(\Gamma_C)$.

Using the Bochner integral theory, we can study Sobolev spaces involving time. We use the spaces $L^p(I;X)$, $1 \leq p \leq \infty$, with a real Banach space X. Continuous functions in time form the space $C(I;X)$. If X is a Hilbert space with scalar product $(\cdot,\cdot)$, then the space-time scalar product is denoted by $((u,v)) := \int_I (u(t),v(t))\, dt$. In general, an outer parenthesis denotes the integration over I. We will use the spaces

$$U := \left\{ \psi \in L^2\left(I;\mathcal{H}_D^1\right) \,\middle|\, \dot{\psi} \in L^2\left(I;\mathcal{H}^{-1}\right) \right\} \quad \text{and} \quad V := \left\{ \chi \in L^2\left(I;\mathcal{L}^2\right) \,|\dot{\chi} \in L^2\left(I;\mathcal{H}^{-1}\right) \right\}.$$

Note that functions u, which are contained in U or V, are continuous in time after possibly being redefined on a set of measure zero. More precisely, they belong to the space $C\left(I;\mathcal{H}^{-1}\right)$, see [19, Theorem 2 in §5.9.2]. Furthermore, we set $\Lambda := L^2\left(I;\tilde{H}_+^{-1/2}(\Gamma_C)\right)$.

The bilinear form of linear elasticity is given by $a(\cdot,\cdot) := (\sigma(\cdot),\varepsilon(\cdot))$. It is continuous and due to Korn's inequality also elliptic. Based on a, the space-time bilinear form A is given by

$$\begin{aligned} A(w,\varphi) \;:=\; & ((v,\psi)) - (\langle \dot{u},\psi\rangle) + (\langle \dot{v},\chi\rangle) + (a(u,\chi)) - ((f,\chi)) \\ & + \langle u(0),\chi(0)\rangle - (u_s,\chi(0)) + \langle v(0),\psi(0)\rangle - (v_s,\psi(0)), \end{aligned}$$

for $w = (u,v) \in W$ and $\varphi = (\chi,\psi) \in W$ with $W := U \times V$. The first two terms in A express the weak equality between the velocity v and the first derivative of u. The remaining terms in the first line are the weak form of the equation of motion. The second line includes the initial conditions in a weak sense. Furthermore, we assume $f \in L^2\left(I;\mathcal{L}^2\right)$, $u_s \in \mathcal{H}_D^1$, $v_s \in \mathcal{L}^2$, and $g \in L^2\left(I;H^{1/2}(\Gamma_C)\right)$ with $\dot{g} \in L^2\left(I;H^{1/2}(\Gamma_C)\right)$.

Finally the weak form of the dynamic contact problem reads:

Definition 1. The functions $(w, \lambda) = ((u, v), \lambda) \in W \times \Lambda$ are a weak solution of the dynamic contact problem, if and only if

$$\forall \varphi = (\chi, \psi) \in W : \qquad A(w, \varphi) + (\langle \lambda, \gamma_n(\chi) \rangle) = 0 \tag{12}$$

$$\forall \mu \in \Lambda : \qquad (\langle \mu - \lambda, \gamma_n(u) - g \rangle) \leq 0 \tag{13}$$

holds.

Mixed formulations of the dynamic contact problem and their equivalence to a variational inequality formulation are discussed, e.g., in [3, 40]. In particular, the equality of σ_{nn} and λ_n is considered. A further variational inequality formulation is discussed in [46], where the equivalence of the strong and the weak formulation is considered. It should be remarked that the existence and uniqueness of a solution u for the purely elastic dynamic Signorini problem is to the best of the authors knowledge an open question. In [2] the existence of a weak solution for the dynamic linear viscoelastic Signorini problem is shown.

One main property of dynamic contact problems is the conservation of the total energy

$$E_{\text{tot}}(t) := E_{\text{kin}}(t) + E_{\text{pot}}(t) := \frac{1}{2}(v(t), v(t)) + \frac{1}{2}a(u(t), u(t)).$$

Proposition 2. *If the right hand side f is zero, the obstacle g does not depend on time, i. e. $\dot{g} \equiv 0$, $(\dot{u}, \dot{v}) \in W$,*

$$\langle u(0), \dot{u}(0) \rangle - (u_s, \dot{u}(0)) + \langle v(0), \dot{v}(0) \rangle - (v_s, \dot{v}(0)) = 0,$$

and the generalized persistency condition

$$(\langle \lambda, \gamma_n(\dot{u}) \rangle) = (\langle \lambda, \gamma_n(\dot{u}) - \dot{g} \rangle) = 0 \tag{14}$$

for a. e. $t \in I$ holds, then the total energy is conserved.

Proof. We test equation (12) with $\varphi := (\dot{u}, \dot{v})$ and obtain

$$\begin{aligned} 0 &= A(w, \varphi) + (\langle \lambda, \gamma_n(\dot{u}) \rangle) = ((v, \dot{v})) + (a(u, \dot{u})) \\ &= \int_0^T \frac{\partial}{\partial t} \frac{1}{2}(v, v) + \frac{\partial}{\partial t} \frac{1}{2} a(u, u)\, dt \\ &= E_{\text{kin}}(T) - E_{\text{kin}}(0) + E_{\text{pot}}(T) - E_{\text{pot}}(0) \\ &= E_{\text{tot}}(T) - E_{\text{tot}}(0). \end{aligned}$$

By varying the endpoint in time T, we obtain that the total energy is constant. □

Remark 3. The linear and the angular momentum are also conserved under suitable assumptions, see for instance [36].

While the first two assumptions of Proposition (2) arise from physical reasons, the third and fourth one are smoothness assumptions on the weak solution (u, v). The generalized persistency condition (14) is a weak version of (9). It corresponds to the pointwise persistency condition due to the sign conditions in (10-11), cf. [32]. However, the generalized persistency condition is not directly included in the weak formulation (12-13) but implicitly as shown in the following proposition, compare [32, Theorem 1.4.2].

Proposition 4. *If $(w, \lambda) \in W \times \Lambda$ is a weak solution of (12-13), $u \in C^1\left(I; \mathcal{H}^1_D\right)$, and $g \in C^1\left(I; H^{1/2}(\Gamma_C)\right)$, then the generalized persistency condition* (14) *holds.*

PROOF. By setting $\mu = 0$ and $\mu = 2\lambda$ in (13), we obtain

$$(\langle \lambda(t), \gamma_n(u(t)) - g(t) \rangle) = 0.$$

Furthermore, since $\lambda \in \Lambda$ and $(\gamma_n(u(t+h)) - g(t+h)) \in H_-^{1/2}(\Gamma_C)$, we also have

$$(\langle \lambda(t), \gamma_n(u(t+h)) - g(t+h) \rangle) \leq 0.$$

repectively

$$\left(\left\langle \lambda(t), \frac{1}{h} \left[\gamma_n(u(t+h) - u(t)) - (g(t+h) - g(t)) \right] \right\rangle \right) \begin{cases} \geq 0, & \text{for } h < 0, \\ \leq 0, & \text{for } h > 0. \end{cases}$$

Finally, we end up with

$$(\langle \lambda, \gamma_n(\dot{u}) - \dot{g} \rangle) = \lim_{h \to 0} \left(\left\langle \lambda(t), \frac{1}{h} \left[\gamma_n(u(t+h) - u(t)) - (g(t+h) - g(t)) \right] \right\rangle \right) = 0.$$

□

3 Discretization

In this section, we discuss the discretisation scheme and show some properties of it. The chosen ansatz is a Petrov-Galerkin scheme, with continuous basis functions in space and time for the displacement and the velocity. The Lagrange multiplier is discretized with piecewise discontinuous functions in space and time. As usual in mixed methods, special attention has to be paid to the balancing of the discretisation of the primal and the dual variable.

The temporal discretisation is based on a decomposition of the time interval $I = [0, T]$ into $M_k \in \mathbb{N}$ subintervals $I_m = (t_{m-1}, t_m]$ with

$$0 = t_0 < t_1 < \ldots < t_{M_k} = T \quad \text{and} \quad I = \{0\} \cup I_1 \cup \ldots \cup I_{M_k}.$$

We work with an equidistant decomposition of the time interval, i.e. the constant time step length is given by $k = {}^{T}/_{M_k}$ and it holds $t_i = ik$. The time instances t_i, $0 \leq i \leq M_k$ correspond to the time steps in a finite difference approach. We also call this decomposition the temporal mesh $\mathbb{T}_k$. By the time step m, we denote the step from t_{m-1} to t_m.

The basic domain Ω is triangulated by a mesh $\mathbb{T}_h$ of quadraliteral or hexahedral elements. The number of mesh elements in the mesh $\mathbb{T}_h$ is denoted by M_h. The mesh does not change over the calculation. The spatial finite element space is

$$V_h := \left\{ \varphi \in \mathcal{H}^1 \,\middle|\, \forall \mathcal{T} \in \mathbb{T}_h : \varphi_{|\mathcal{T}} \in Q_{p_s}\left(\mathcal{T}; \mathbb{R}^d\right) \right\}.$$

Here, $Q_{p_s}\left(\mathcal{T}; \mathbb{R}^d\right)$ is the set of d-polynomial basis functions of degree p_s on a mesh cell $\mathcal{T}$.

The temporal test space is defined as

$$W_{kh} := \left\{ \varphi_{kh} \in L^2\left(I; \mathcal{H}^1\right) \,\middle|\, \varphi_{kh|I_m} \in \mathcal{P}_{p_t - 1}\left(I_m; V_h\right),\ m = 1, 2, \ldots, M_k,\ \varphi_{kh}(0) \in V_h \right\}.$$

Here, $\mathcal{P}_{p_t}(\omega; X)$ is the linear space of polynomials on $\omega \subset \mathbb{R}$ with values in X, which have the maximum degree p_t. Functions from W_{kh} are possibly discontinuous at t_i, $i = 0, 1, \ldots, M_k$. The temporal trial space is given by

$$V_{kh} := \left\{ \varphi_{kh} \in C\left(I; \mathcal{H}^1\right) \,\middle|\, \varphi_{kh|I_m} \in \mathcal{P}_{p_t}\left(I_m; V_h\right),\ m = 1, 2, \ldots, M_k \right\}.$$

Corresponding continuous space-time Galerkin methods for the wave equation are analyzed for instance in [4, 20].

The discrete Lagrange multipliers are defined on the boundary mesh $\mathbb{B}_H$ representing the contact boundary Γ_C and on the temporal mesh $\mathbb{T}_K$. The indices H and K indicate that coarser meshes may be chosen for the Lagrange multiplier in space and time. We assume here that $K = nk$, $n \in \mathbb{N}$ and $M_k \mod n = 0$. Let $M_K = {}^{M_k}/_n$ and $J_m = ((m-1)K, mK]$. The spatial trial and test set for the Lagrange multiplier is

$$\Lambda_H := \left\{ \mu \in L^2(\Gamma_C) \,\middle|\, \forall \mathcal{T} \in \mathbb{B}_H : \mu_{|\mathcal{T}} \in \mathcal{P}_{q_s}(\mathcal{T}, \mathbb{R}),\ \forall \xi \in G(\mathcal{T}) : \mu(\xi) \leq 0 \right\},$$

where $G_{\mathcal{T}}$ is a set of test points. For $q_s = 0$, we take the midpoint as test point. For linear polynomials, we work with the endpoints. This leads to a conforming scheme. For $q_s > 1$, we take the q_s^d Gauß-points on $\mathcal{T}$ as test points. This choice leads to a convergent scheme, cf. [6]. We define the space-time trial and test set by

$$\Lambda_{KH} := \left\{ \mu_{KH} \in L^2\left(I; L^2(\Gamma_C)\right) \,\middle|\, \forall J \in \mathbb{T}_K : \mu_{KH|I} \in \mathcal{P}_{q_t}(J; \Lambda_H) \right\}.$$

The discretisation reads:

Definition 5. The functions $(w_{kh}, \lambda_{KH}) = ((u_{kh}, v_{kh}), \lambda_{KH}) \in (V_{kh} \times V_{kh}) \times \Lambda_{KH}$ are a discrete solution of the dynamic contact problem, if and only if

$$A_{kh}(w_{kh}, \varphi_{kh}) + ((\lambda_{KH}, \gamma_n(\varphi_{kh}))) = 0 \tag{15}$$

$$\left((\mu_{KH} - \lambda_{KH}, \gamma_n(u_{kh}) - g_{kh})_{\Gamma_C} \right) \leq 0 \tag{16}$$

holds, where equation (15) has to be valid for all $\varphi_{kh} = (\psi_{kh}, \chi_{kh}) \in W_{kh} \times W_{kh}$ and inequality (16) for all $\mu_{KH} \in \Lambda_{KH}$. The discrete space-time bilinear form is

$$\begin{aligned} A_{kh}(w_{kh}, \varphi_{kh}) = & \sum_{m=1}^{M_k} \left\{ ((v_{kh} - \dot{u}_{kh}, \psi_{kh}))_{I_m} + ((\dot{v}_{kh}, \chi_{kh}))_{I_m} \right\} \\ & + \sum_{m=1}^{M_k} \left\{ (a(u_{kh}, \chi_{kh}))_{I_m} - ((f, \chi_{kh}))_{I_m} \right\} \\ & + \left(u_{kh}^0 - u_s, \chi_{kh}^0\right) + \left(v_{kh}^0 - v_s, \psi_{kh}^0\right). \end{aligned}$$

Furthermore, g_{kh} is the projection of g in the trace space of V_{kh}.

We have discretized the dymanic contact problem in the usual "finite element way". Thus, we expect as usual that the properties of the continuous solution carry over to the discrete one. In the following proposition, we discuss the conservation of the total energy:

Proposition 6. *If the right hand side f is zero, $\dot{g}$ vanishes, and the discrete persistency condition*

$$\left((\lambda_{KH}, \gamma_n(\dot{u}_{kh}) - \dot{g}_{kh})_{\Gamma_C} \right)_J = 0 \tag{17}$$

for all $J \in \mathbb{T}_K$ holds, then the total energy is constant on all time instances in $\mathbb{T}_K$.

Remark 7. The energy conservation can be disturbed by adaptive methods and one has to pay attention to this fact, when applying adaptive methods. See, for instance, [42].

PROOF. We are allowed to test equation (15) on a subinterval $J = (t_1, t_2] \in \mathbb{T}_K$ with $(\dot{v}_{kh}, \dot{u}_{kh})$ and obtain

$$\begin{aligned} 0 &= ((v_{kh}, \dot{v}_{kh}))_J + (a(u_{kh}, \dot{u}_{kh}))_J + \left((\lambda_{KH}, \gamma_n(\dot{u}_{kh}))_{\Gamma_C}\right)_J \\ &= \frac{1}{2}\left(v_{kh}^2, v_{kh}^2\right) - \frac{1}{2}\left(v_{kh}^1, v_{kh}^1\right) + \frac{1}{2}a\left(u_{kh}^2, u_{kh}^2\right) \\ &\quad -\frac{1}{2}a\left(u_{kh}^1, u_{kh}^1\right) + \left(\left(\lambda_{KH}, \gamma_n\left(\dot{u}_{kh}\right)\right)_{\Gamma_C}\right)_J. \end{aligned}$$

Consequently, it holds

$$E_{tot}^2 - E_{tot}^1 = -\left(\left(\lambda_{KH}, \gamma_n\left(\dot{u}_{kh}\right)\right)\right)_J = 0.$$

□

For the discrete persistency condition, we obtain

Proposition 8. *The discrete persistency condition holds in the limit case, i.e.*

$$\lim_{K\to 0} \frac{1}{K}\left(\left(\lambda_{KH}(t), \gamma_n\left(u_{kh}(t+K) - u_{kh}(t)\right) - g_{kh}(t+K) + g_{kh}(t)\right)_{\Gamma_C}\right)_J = 0$$

for $J \in \mathbb{T}_K$.

Remark 9. Here, we demand that the contact conditions are strictly fulfilled in the integral mean value over space and time. If we pass on this demand and require the contact conditions only in the limit case $K \to 0$, we are able to ensure a discrete persistency condition. We refer to [36] for this well known proceeding.

PROOF. By setting $\mu_{KH} = 0$ and $\mu_{KH} = 2\lambda_{KH}$ in (16), we obtain

$$\left(\left(\lambda_{KH}, \gamma_n\left(u_{kh}\right) - g_{kh}\right)_{\Gamma_C}\right)_J = 0.$$

The test function $\mu_{KH}(t) = \lambda_{KH}(t + \alpha K) + \lambda_{KH}(t)$, $\alpha \in \mathbb{Z}$, leads to

$$\begin{aligned} &\left(\left(\lambda_{KH}(t+\alpha K) + \lambda_{KH}(t) - \lambda_{KH}(t+\alpha K), \gamma_n\left(u_{kh}(t+\alpha K)\right) - g_{kh}(t+\alpha K)\right)_{\Gamma_C}\right)_J \\ = &\left(\left(\lambda_{KH}(t), \gamma_n\left(u_{kh}(t+\alpha K)\right) - g_{kh}(t+\alpha K)\right)_{\Gamma_C}\right)_J \leq 0, \end{aligned}$$

repectively

$$\left(\left(\lambda_{KH}(t), \frac{1}{\alpha K}\left[\gamma_n\left(u_{kh}(t+\alpha K) - u_{kh}(t)\right) - g_{kh}(t+\alpha K) + g_{kh}(t)\right]\right)_{\Gamma_C}\right)_J$$

$$\begin{cases} \geq 0, & \text{for } \alpha < 0, \\ \leq 0, & \text{for } \alpha > 0, \end{cases}$$

which implies the assertion. □

4 Solution of the discrete problem

In the last section, we have presented the space-time Galerkin discretization. It leads to a discrete problem in space and time, which has to be solved numerically. To this end, we choose the temporal test functions such that the single time steps w.r.t. the temporal mesh $\mathbb{T}_K$ decouple. Furthermore, we seperate the equation defining the balance of momentum and the definition of the velocity field v. Thus, we obtain the time stepping scheme:

Time Stepping Scheme 1. Find $w_{kh} = (u_{kh}, v_{kh}) \in V_{kh} \times V_{kh}$ and $\lambda_{KH} \in \Lambda_{KH}$, where $w_{kh}^0 \in V_h \times V_h$ is given by

$$\begin{aligned} \forall \psi_h \in V_h: \quad \left(u_{kh}^0 - u_s, \psi_h\right) &= 0, && (18)\\ \forall \chi_h \in V_h: \quad \left(v_{kh}^0 - v_s, \chi_h\right) &= 0. && (19) \end{aligned}$$

For $m = 1, 2, \ldots, M_K$, $w_{kh|J_m} \in V_{kh|J_m} \times V_{kh|J_m}$ and $\lambda_{KH|J_m} \in \Lambda_{KH|J_m}$ are the solution of the system

$$\begin{aligned} \left((v_{kh} - \dot{u}_{kh}, \psi_{kh})\right)_{J_m} &= 0, && (20)\\ \left((\dot{v}_{kh}, \chi_{kh})\right)_{J_m} + \left(a\left(u_{kh}, \chi_{kh}\right)\right)_{J_m} + \left((\lambda_{KH}, \gamma_n\left(\varphi_{kh}\right))\right)_{J_m} &= \left((f, \chi_{kh})\right)_{J_m}, && (21)\\ \left((\mu_{KH} - \lambda_{KH}, \gamma_n\left(u_{kh}\right) - g_{kh})\right)_{J_m} &\leq 0, && (22) \end{aligned}$$

which has to hold for all $\psi_{kh}, \chi_{kh} \in V_{kh|J_m}$ and all $\mu_{KH} \in \Lambda_{KH|J_m}$.

The equations (18) and (19) correspond to L^2-projections into the discrete spatial trial space, which are easy to solve. If u_s and v_s are smooth enough, we can also use the interpolations of u_s and v_s. The solution of the system (20-22) is more involved. First of all, we specifiy our temporal degrees of freedom. Since we use a continuous ansatz in time and evaluate the temporal integrals by Gauß-Lobatto-quadrature-rules, they are chosen as the p_t Gauß-Lobatto-points. For the discontinuous Lagrange multipliers, we work with the Gauß-Radau-quadrature-points as temporal degrees of freedom.

The coefficients of a spatial finite element function $x_h \in V_h$ are collected in a vector named $\hat{x}$. Based on this spatial data, we define the vector

$$\tilde{x}^m = \left(\left(\hat{x}^{m,1}\right)^\top, \left(\hat{x}^{m,2}\right)^\top, \ldots, \left(\hat{x}^{m,p_t}\right)^\top\right)^\top,$$

which represents the coefficients of a function $x_{kh} \in V_{kh}$ on the time intervall I_m. The coefficients of $x_{kh} \in V_{kh}$ on the time interval J_m are stored in the vector

$$\bar{x}^m = \left(\left(\tilde{x}^{(m-1)n+1}\right)^\top, \left(\tilde{x}^{(m-1)n+2}\right)^\top, \ldots, \left(\tilde{x}^{mn}\right)^\top\right)^\top.$$

Thus, we can identify the functions u_{kh} and v_{kh} with the vectors $\bar{u}^m$ and $\bar{v}^m$, $m = 1, 2, \ldots, M_K$, respectively. Furthermore, $\left((f, \chi_{kh})\right)_{J_m}$ corresponds to an assembled vector $\bar{f}^m$ and $\left((\mu_{KH}, g_{kh})\right)_{J_m}$ to $\bar{g}^m$. The vector representing $\lambda_{KH} \in \Lambda_{KH}$ on J_m is given by

$$\bar{\lambda}^m = \left(\left(\hat{\lambda}^{m,1}\right)^\top, \left(\hat{\lambda}^{m,2}\right)^\top, \ldots, \left(\hat{\lambda}^{m,q_t}\right)^\top\right)^\top.$$

With this notation, the equations (20) and (21) can be written in algebraic form as

$$\begin{pmatrix} M & -\dot{M} & 0 \\ \dot{M} & K & \tilde{N} \end{pmatrix} \begin{pmatrix} \bar{v}^m \\ \bar{u}^m \\ \bar{\lambda}^m \end{pmatrix} = \begin{pmatrix} 0 \\ \bar{f}^m \end{pmatrix},$$

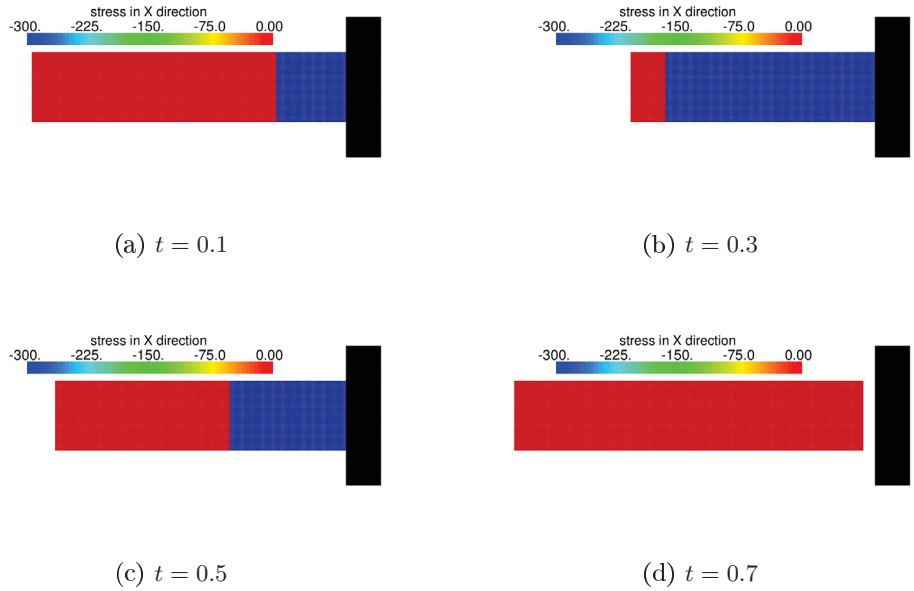

(a) $t = 0.1$ (b) $t = 0.3$

(c) $t = 0.5$ (d) $t = 0.7$

Fig. 1: Analytic stress distribution in Ω for different time instances

where the matrix M corresponds to $((\chi_{kh}, \psi_{kh}))_{J_m}$, $\dot{M}$ to $((\dot{\chi}_{kh}, \psi_{kh}))_{J_m}$, K to $(a(\chi_{kh}, \psi_{kh}))$, and $\tilde{N}$ to $((\mu_{kh}, \gamma_n(\psi_{kh})))_{J_m}$. By setting

$$A := \begin{pmatrix} M & -\dot{M} \\ \dot{M} & K \end{pmatrix}, \; N := \begin{pmatrix} 0 \\ \tilde{N} \end{pmatrix}, \; \bar{w}^m := \begin{pmatrix} \bar{v}^m \\ \bar{u}^m \end{pmatrix}, \; \bar{r}^m := \begin{pmatrix} 0 \\ \bar{f}^m \end{pmatrix},$$

we obtain the simplified form

$$A\bar{w}^m + N\bar{\lambda}^m = \bar{r}^m. \tag{23}$$

It should be remarked that the matrix A is not symmetric positive definite due to the chosen Petrov-Galerkin-discretization. The inequality (22) can be written as

$$\left(\bar{\mu} - \bar{\lambda}^m\right)^\top \left(N^\top \bar{w}^m - \bar{g}^m\right) \leq 0 \tag{24}$$

for all admissible coefficients $\bar{\mu}$. The system (23-24) has the same structure as static contact problems. Consequently, the same solution techniques can be used. Here, we apply the algorithms introduced in [7], which are based on the primal-dual active set strategy, see for instance [25, 26].

5 Numerical results

In this section, we test the presented discretization by a benchmark problem. We consider a 2d version of an example given in [18]: The domain is $\Omega := (-h_0 - L, -h_0) \times (0, 2)$, $h_0 = 0.1$, $L = 10$, and the time interval $I = [0, 0.8]$. We set $E = 900$, $\nu = 0$, and $\rho \equiv 1$. As possible contact boundary, we choose $\Gamma_C = \{-h_0\} \times [0, 2]$. Furthermore, we prescribe only homogeneous Neuman boundary conditions, i.e. $\Gamma_D = \emptyset$ and $\Gamma_N = \partial\Omega \backslash \Gamma_C$. We have an initial displacement $u_s \equiv 0$ and an initial velocity $v_s \equiv (v_0, 0)^\top$, $v_0 = 10$. The gap function is given by $g \equiv h_0$. From the specific velocity $c_0 = \sqrt{E/\rho} = 30$, we obtain the time $\tau_w = v_0/c_0 = 1/3$, which a stress wave needs to travel through Ω. Thus, the impact time is $t_1 = h_0/v_0 = 0.01$ and

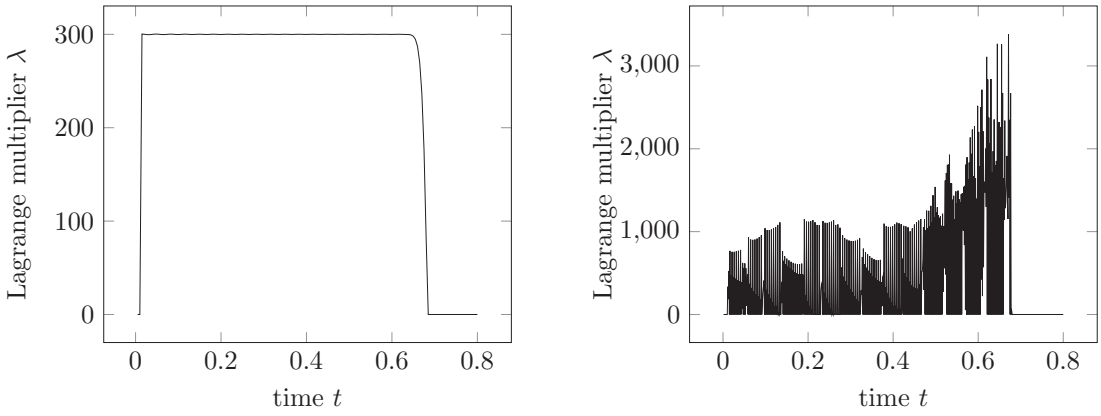

(a) $M_K = 160$ (b) $M_K = 640$

Fig. 2: Plot of the Lagrange multiplier λ_{KH} for $H = 2h$, $K = 2k$, $p_t = p_s = 1$, $q_t = q_s = 0$, $M_h = 20480$ and different number of time steps

	$M_K = 80$	$M_K = 160$	$M_K = 320$	$M_K = 640$
$M_h = 1280$	stable	unstable	unstable	unstable
$M_h = 5120$	stable	stable	unstable	unstable
$M_h = 20480$	stable	stable	stable	unstable

Tab. 1: Stability test for $p_s = p_t = 1$, $q_s = q_t = 0$, $H = 2h$, $K = 2k$

the time for loosing contact is $t_2 = t_1 + 2\tau_w = {}^{203}/_{300}$. The analytic displacement $u := (u_1, 0)$ is then given by

$$u_1(x_1, x_2, t) := \begin{cases} v_0 t, & t \le t_1 \\ h_0 + v_0 \min\left\{-\frac{h_0+x_1}{c_0}, \tau_w - |t - t_1 - \tau_w|\right\}, & t_1 < t \le t_2 \\ h_0 - v_0 (t - t_2), & t_2 < t \end{cases},$$

the analytic velocity $v := (v_1, 0)$ by

$$v_1(x_1, x_2, t) := \begin{cases} v_0, & t \le t_1 \\ 0, & t_1 < t \le t_2,\ -\frac{h_0+x_1}{c_0} \le \tau_w - |t - t_1 - \tau_w| \\ -v_0 \operatorname{sign}(t - t_1 - \tau_w), & t_1 < t \le t_2,\ -\frac{h_0+x_1}{c_0} > \tau_w - |t - t_1 - \tau_w| \\ -v_0, & t_2 < t \end{cases},$$

as well as the normal contact stress by

$$\sigma_{nn}(x_2, t) = \lambda(x_2, t) = \begin{cases} 0, & t < t_1, t > t_2 \\ -\frac{E v_0}{c_0} = -300, & \text{else} \end{cases}. \tag{25}$$

The analytical solution is illustrated in Figure 1.

We applied our approach with different parameters on the presented example. In Figure 2, the Lagrange multiplier λ_{KH} is plotted over the time interval I. Since λ_{KH} is constant on Γ_C in every time step, we can neglect the spatial dependence. In Figure 2(a), the Lagrange multiplier coincides with the analytic contact stress given in (25) and show no oscillations at all. However, if we use a smaller time step size, large oscillations are observed, see Figure 2(b). This is a typical behavior, which can be seen for different parameters. In particular, we observe such instabilities for $p_t = q_t$ and $K = 2k$ as well as for $p_t - 1 = q_t$ and $K = k$.

	$M_K = 80$	$M_K = 160$	$M_K = 320$	$M_K = 640$
$M_h = 1280$	stable	unstable	unstable	unstable
$M_h = 5120$	stable	stable	unstable	unstable
$M_h = 20480$	stable	stable	stable	unstable

Tab. 2: Stability test for $p_s = 2$, $p_t = 1$, $q_s = 1$, $q_t = 0$, $H = 2h$, $K = 2k$

	$M_K = 80$	$M_K = 160$	$M_K = 320$	$M_K = 640$
$M_h = 1280$	stable	unstable	unstable	unstable
$M_h = 5120$	stable	stable	unstable	unstable
$M_h = 20480$	stable	stable	stable	unstable

Tab. 3: Stability test for $p_s = 3$, $p_t = 1$, $q_s = 2$, $q_t = 0$, $H = 2h$, $K = 2k$

	$M_K = 80$	$M_K = 160$	$M_K = 320$	$M_K = 640$
$M_h = 1280$	stable	unstable	unstable	unstable
$M_h = 5120$	stable	stable	unstable	unstable
$M_h = 20480$	stable	stable	stable	unstable

Tab. 4: Stability test for $p_s = 1$, $p_t = 2$, $q_s = 0$, $q_t = 0$, $H = 2h$, $K = k$

	$M_K = 80$	$M_K = 160$	$M_K = 320$	$M_K = 640$
$M_h = 1280$	stable	unstable	unstable	unstable
$M_h = 5120$	stable	stable	unstable	unstable
$M_h = 20480$	stable	stable	stable	unstable

Tab. 5: Stability test for $p_s = 1$, $p_t = 2$, $q_s = 0$, $q_t = 1$, $H = 2h$, $K = 2k$

	$M_K = 80$	$M_K = 160$	$M_K = 320$	$M_K = 640$
$M_h = 1280$	0.13%	1318%	2760%	6114%
$M_h = 5120$	0.053%	0.076%	1205%	4205%
$M_h = 20480$	0.093%	0.019%	0.049%	1302%

Tab. 6: Energy deviation for $p_s = p_t = 1$, $q_s = q_t = 0$, $H = 2h$, $K = 2k$

We study the parameter dependence in more detail. To this end, the problem is numerically solved with different parameters. In Table 1, the parameters $p_t = p_s = 1$, $q_s = q_t = 0$, $H = 2h$, and $K = 2k$ are considered. We observe stable behavior for all time step sizes K with $K \geq Ch$ or $M_K \leq \bar{C}\sqrt{M_h}$. Table 2 and3 show that the stability does not depend on p_s and q_s, i.e. the degree of the spatial basis functions is not relevant. In the Tables 4 and 5, quadratic basis functions in time for the velocity and the displacement ($p_t = 2$) are tested. At first, we combine them with piecewise constant Lagrange multiplier on the same mesh, i.e. $q_t = 0$ and $K = k$. This approach leads to the same stability properties just like the approach based on $q_t = 1$ and $K = 2k$. Thus, both approaches to stabilize lead to stable schemes. In Table 6, the energy deviation at the end of the calculation is outlined. We find a large energy increase in the case of instability. Otherwise the energy deviation is smaller than 1%.

6 Conclusions and outlook

In this article, we present a space-time Galerkin method for dynamic Signorini problems. We found in our numerical study that our approach is stable, if the temporal discretization fulfills the assumptions, which are known from the space discretization. However, it turns out that the time step length is bounded below to ensure stability. Here, the lower bound is given by Ch. Furthermore, the proposed method is only energy conserving for time step size to zero, since it exactly fulfills the contact constraints. Several aspects need further investigations. First of all, it has to be examined, why the method becomes unstable for small time step sizes. Here, an analysis of the stability properties is needed. Further investigations concentrate on adaptive methods to use the full capabilities of the method with respect to convergence rates, which is limited due to the nonsmoothness of the underlying problem for uniform meshes.

Acknowledgement

The author gratefully acknowledges the financial support by the Mercator Research Center Ruhr (MERCUR) within the research project “Space-time finite element methods for thermo-mechanically coupled contact problems” (AN-2013-0060).

References

[1] R. A. Adams. *Sobolev spaces*. Pure and Applied Mathematics. Academic Press, New York, 1975.

[2] J. Ahn and D. E. Stewart. Dynamic frictionless contact in linear viscoelasticity. *IMA J. Numer. Anal.*, 1:43–71, 2009.

[3] F. Armero and E. Petőcz. Formulation and analysis of conserving algorithms for frictionless dynamic contact/impact problems. *Comput. Methods Appl. Mech. Engrg.*, 158:269–300, 1998.

[4] L. Bales and I. Lasiecka. Continuous finite elements in space and time for the nonhomogeneous wave equation. *Comput. Math. Appl.*, 27(3):91–102, 1994.

[5] K. J. Bathe and A. B. Chaudhary. A solution method for static and dynamic analysis of three-dimensional contact problems with friction. *Comput. & Struct.*, 24(6):855–873, 1986.

[6] H. Blum, H. Kleemann, and A. Schröder. Mixed finite element methods for two-body contact problems. *J. Comput. Appl. Math.*, 283:58–70, 2015.

[7] H. Blum, H. Ludwig, and A. Rademacher. Semi-smooth newton methods for mixed fem discretizations of higher-order for frictional, elasto-plastic two-body contact problems. *Ergebnisberichte Angewandte Mathematik, Fakultät für Mathematik, TU Dortmund*, 493, 2014.

[8] H. Blum, A. Rademacher, and A. Schröder. Space adaptive finite element methods for dynamic obstacle problems. *ETNA, Electron. Trans. Numer. Anal.*, 32:162–172, 2008.

[9] H. Blum, A. Rademacher, and A. Schröder. Space adaptive finite element methods for dynamic Signorini problems. *Comput. Mech.*, 44(4):481–491, 2009.

[10] F. Chouly, P. Hild, and Y. Renard. A Nitsche finite element method for dynamic contact: 1. Space semi-discretization and time-marching schemes. *ESAIM: M2AN*, 2014. appeared online, doi: 10.1051/m2an/2014041.

[11] F. Chouly, P. Hild, and Y. Renard. A Nitsche finite element method for dynamic contact: 2. Stability of the schemes and numerical experiments. *ESAIM: M2AN*, 2014. appeared online, doi: 10.1051/m2an/2014046.

[12] J. Chung and G. M. Hulbert. A time integration algorithm for structural dynamics with improved numerical dissipation: The generalized-α method. *J. Appl. Mech.*, 60:371–375, 1993.

[13] A. Czekanski, N. El-Abbasi, and S. A. Meguid. Optimal time integration parameters for elastodynamic contact problems. *Commun. Numer. Math. Engrg.*, 17:379–384, 2001.

[14] R. Dautray and J.-L. Lions. *Mathematical Analysis and Numerical Methods for Science and Technology: Evolution Problems I, Vol. 5.* Springer-Verlag, Berlin, 1992.

[15] P. Deuflhard, R. Krause, and S. Ertel. A contact-stabilized newmark method for dynamical contact problems. *Int. J. Numer. Methods Engrg.*, 73:1274–1290, 2008.

[16] T. Dickopf and R. Krause. Efficient simulation of multi-body contact problems on complex geometries: A flexible decomposition approach using constrained minimization. *Int. J. Numer. Methods Engrg.*, 77(13):1834–1862, 2009.

[17] Z. Dostál, D. Horák, R. Kučera, V. Vondrák, J. Haslinger, J. r. Dobiáš, and S. Pták. FETI based algorithms for contact problems: Scalability, large displacements and 3D Coulomb friction. *Comput. Methods Appl. Mech. Engrg.*, 194(2-5):395–409, 2005.

[18] D. Doyen, A. Ern, and S. Piperno. Time-integration schemes for the finite element dynamic signorini problem. *SIAM J. Sci. Comput.*, 33:223–249, 2011.

[19] L. C. Evans. *Partial Differential Equations.* American Mathematical Society, 1998.

[20] D. A. French and T. E. Peterson. A continuous space-time finite element method for the wave equation. *Math. Comput.*, 65(214):491–506, 1996.

[21] C. Hager, S. Hüeber, and B. Wohlmuth. A stable energy conserving approach for frictional contact problems based on quadrature formulas. *Int. J. Numer. Methods Engrg.*, 73:205–225, 2008.

[22] J. Haslinger, Z. Dostál, and R. Kučera. On a splitting type algorithm for the numerical realization of contact problems with coulomb friction. *Comput. Methods Appl. Mech. Engrg.*, 191(21-22):2261–2281, 2002.

[23] J. Haslinger, R. Kučera, and Z. Dostál. An algorithm for the numerical realization of 3D contact problems with Coulomb friction. *J. Comput. Appl. Math.*, 164-165:387–408, 2004.

[24] J. Haslinger and T. Sassi. Mixed finite element approximation of 3d contact problems with given friction: error analysis and numerical realization. *Math. Mod. Numer. Anal.*, 38:563–578, 2004.

[25] M. Hintermüller, K. Ito, and K. Kunisch. The primal-dual active set strategy as a semi-smooth newton method. *SIAM J. Optim.*, 13(3):865–888, 2003.

[26] S. Hüeber, G. Stadler, and B. I. Wohlmuth. A primal-dual active set algorithm for three-dimensional contact problems with coulomb friction. *SIAM J. Sci. Comput.*, 30(2):572–596, 2008.

[27] Hüeber, S. and Matei, A. and Wohlmuth, B.I. Efficient algorithms for problems with friction. *SIAM J. Sci. Comput.*, 29(1):70–92, 2007.

[28] C. Kane, J. E. Marsden, M. Ortiz, and E. A. Repetto. Finite element analysis of nonsmooth contact. *Comput. Methods Appl. Mech. Engrg.*, 180:1–26, 1999.

[29] J. E. Kane, C amd Marsden, M. Ortiz, and A. Pandolfi. Time-discretized variational formulation of non-smooth frictional contact. *Int. J. Numer. Meth. Engrg.*, 53:1801–1829, 2002.

[30] H. B. Khenous, P. Laborde, and Y. Renard. Mass redistribution method for finite element contact problems in elastodynamics. *Eur. J. Mech. Solids -A/Solids*, 27(5):918–932, 2008.

[31] N. Kikuchi and J. T. Oden. *Contact Problems in Elasticity: A Study of Variational Inequalities and Finite Element Methods.* SIAM, Studies in Applied Mathematics, 1988.

[32] C. Klapproth. *Adaptive Numerical Integration of Dynamical Contact Problems.* PhD thesis, Freie Universität Berlin, 2011.

[33] R. Kornhuber and R. Krause. Adaptive multigrid methods for Signorini's problem in linear elasticity. *Comput. Vis. Sci.*, 4(1):9–20, 2001.

[34] R. Krause and M. Walloth. A time discretization scheme based on rothe's method for dynamical contact problems with friction. *Comput. Methods Appl. Mech. Engrg.*, 199(1-4):1 – 19, 2009.

[35] R. Krause and M. Walloth. Presentation and comparison of selected algorithms for dynamic contact based on the newmark scheme. *Appl. Numer. Math.*, 62:1393–1410, 2012.

[36] T. A. Laursen. *Computational Contact and Impact Mechanics.* Springer, Berlin Heidelberg New York, 2002.

[37] T. A. Laursen and V. Chawla. Design of energy conserving algorithms for frictionless dynamic contact problems. *Int. J. Numer. Methods Engrg.*, 40:863–886, 1997.

[38] T. W. McDevitt and T. A. Laursen. A mortar-finite element formulation for frictional contact problems. *Int. J. Numer. Methods Engrg.*, 48:1525–1547, 2000.

[39] N. M. Newmark. A method of computation for structural dynamics. *J. Engrg. Mech. Div.-ASCE*, 85(EM3):67–94, 1959.

[40] P. Papadopoulos and R. L. Taylor. On a finite element method for dynamic contact/impact problems. *Int. J. Numer. Methods Engrg.*, 36:2123–2140, 1993.

[41] M. Puso and T. A. Laursen. A 3d contact smoothing method using gregory patches. *Int. J. Numer. Methods Engrg.*, 54:1161–1194, 2002.

[42] A. Rademacher. *Adaptive Finite Element Methods for Nonlinear Hyperbolic Problems of Second Order*. PhD thesis, Technische Universität Dortmund, 2009.

[43] A. Rademacher, A. Schröder, H. Blum, and H. Kleemann. Mixed fem of higher-order for time-dependent contact problems. *Appl. Math. Comput.*, 233:165–186, 2014.

[44] A. Schröder, H. Blum, A. Rademacher, and H. Kleemann. Mixed FEM of higher order for contact Problems with friction. *Int. J. Numer. Anal. Model.*, 8(2):302–323, 2011.

[45] E. Stein, T. Vu Van, and P. Wriggers. Finite element formulation of large deformation impact-contact problems with friction. *Comput. Struct.*, 37(3):319–331, 1990.

[46] D. Talaslidis and P. D. Panagiotopoulos. A linear finite element approach to the solution of the variational inequalities arising in contact problems of structural dynamics. *Int. J. Numer. Methods Engrg.*, 18:1505–1520, 1982.

[47] K. Weinert, H. Blum, T. Jansen, and A. Rademacher. Simulation based optimization of the NC-shape grinding process with toroid grinding wheels. *Prod. Engrg.*, 1:245–252, 2007.

[48] B. I. Wohlmuth and R. H. Krause. Monotone multigrid methods on nonmatching grids for nonlinear multibody contact problems. *SIAM J. Sci. Comput.*, 25(1):324–347, 2003.

[49] P. Wriggers. *Computational Contact Mechanics*. John Wiley & Sons Ltd, Chichester, 2002.